Supplement of Biogeosciences, 21, 3641–3663, 2024
https://doi.org/10.5194/bg-21-3641-2024-supplement

Biogeosciences Open Access EGU

Supplement of

Technical note: A Bayesian mixing model to unravel isotopic data and quantify trace gas production and consumption pathways for time series data – Time-resolved FRactionation And Mixing Evaluation (Time-FRAME)

Eliza Harris et al.

Correspondence to: Eliza Harris (eliza.harris@unibe.ch)

S1 Fractionation followed by mixing, or mixing followed by fractionation?

We simulated N_2O isotopic composition using the endmembers given in Table 1 of the main article to explore differences between the two scenarios (SI Figures S1 and S2):

1. **Mixing followed by fractionation due to reduction (MR)**:

$$\delta_{MR} = f_D\delta_D + f_N\delta_N + \epsilon\ln(r) \tag{S1}$$

where D = denitrification, N = nitrification and r = fraction of total N_2O remaining following reduction

2. **Fractionation due to reduction followed by mixing (RM)**:

$$\delta_{RM} = (f_D \times r_D)(\delta_D + \epsilon\ln(r_D)) + f_N\delta_N \tag{S2}$$

where r_D is the fraction of N_2O from denitrification remaining after reduction, whereby $r_D = \frac{r}{f_D}$ (SI Figure S1).

In the RM scenario, r cannot be larger than the f_D, or r_D would be > 1, which implies at least some degree of mixing before fractionation. The 1σ uncertainty in resulting isotopic composition was estimated using error propagation with the 1σ uncertainties in δ_D, δ_N and ϵ as given in Table 1 of the main article.

Comparing these simulations show that both scenarios deliver the same general trend, whereby isotopic composition increases as the fraction of N_2O remaining following reduction decreases. In both cases, there is a significant difference between the scenarios only when the fraction of N_2O remaining is very low. For N_2O, the major uncertainty is contributed by the isotopic endmembers rather than the fractionation model; isotopic endmembers for different source or emission categories are similarly uncertain for other trace gases such as CH_4 Eyer et al. (2016); Röckmann et al. (2016). This is further shown in the 'boma' case study, where static source apportionment using the MR and RM models gave very similar results (Section 4.3 of the main article). Studies show that a large proportion of the range in endmember values is due to true variability rather than measurement uncertainty, for example due to different rate-limiting steps and microbial enzymes under different conditions, thus even with instrumental development, the endmembers are likely to continue to contribute this level of uncertainty Yu et al. (2020) except in specific cases such as pure culture studies.

For TimeFRAME, we opt to use the MR model rather than the RM model. In reality, mixing and fractionation are occurring simultaneously, however to represent this in a model would add an extra level of complexity that would introduce too many degrees of freedom to be constrained with isotopic data timeseries. The MR model is a better approximation of the 'true' situation, because it is clear mixing occurs to some degree in real scenarios. This is illustrated for example by observations of net N_2O uptake, showing N_2O produced by other pathways is consumed in complete denitrification. Moreover, many microbes producing N_2O by denitrification cannot produce nitrous oxide reductase, thus in this case mixing must occur before reduction and Eq. S2 does not apply. Users of TimeFRAME should exercise caution in the interpretation of results when the fraction of N_2O (or other trace gas) remaining is very low, and when other factors suggest that reduction before mixing could be predominant.

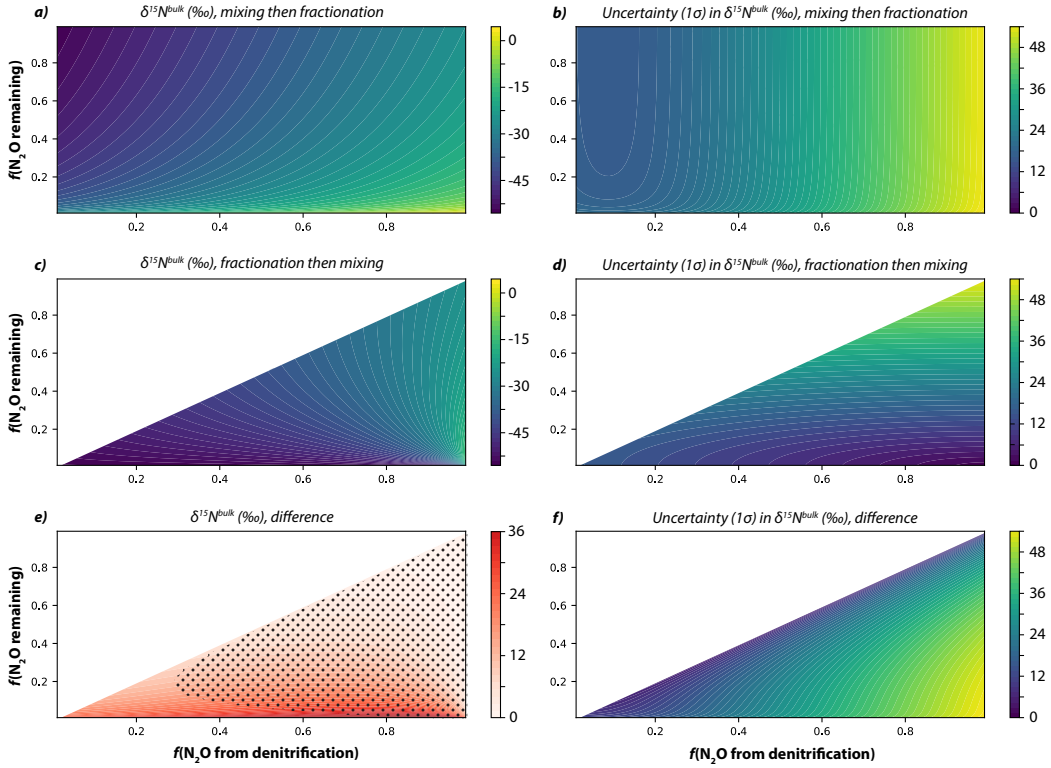

Figure S1. $\delta^{15}\mathrm{N}^{\mathrm{bulk}}$ values simulated across a range of 0 to 1 for the contribution of denitrification to N_2O production (contribution of nitrification = 1 - f(N_2O from denitrification) and 0 to 1 for the fraction of N_2O remaining after consumption. a) and b) show $\delta^{15}\mathrm{N}^{\mathrm{bulk}}$ and its uncertainty simulated with SI Eq. S1. c) and d) show $\delta^{15}\mathrm{N}^{\mathrm{bulk}}$ and its uncertainty simulated with SI Eq. S2. e) and f) show the absolute difference in $\delta^{15}\mathrm{N}^{\mathrm{bulk}}$ between the two simulations and its uncertainty. The dotted region in e) indicates where there is no significant difference between the two scenarios.

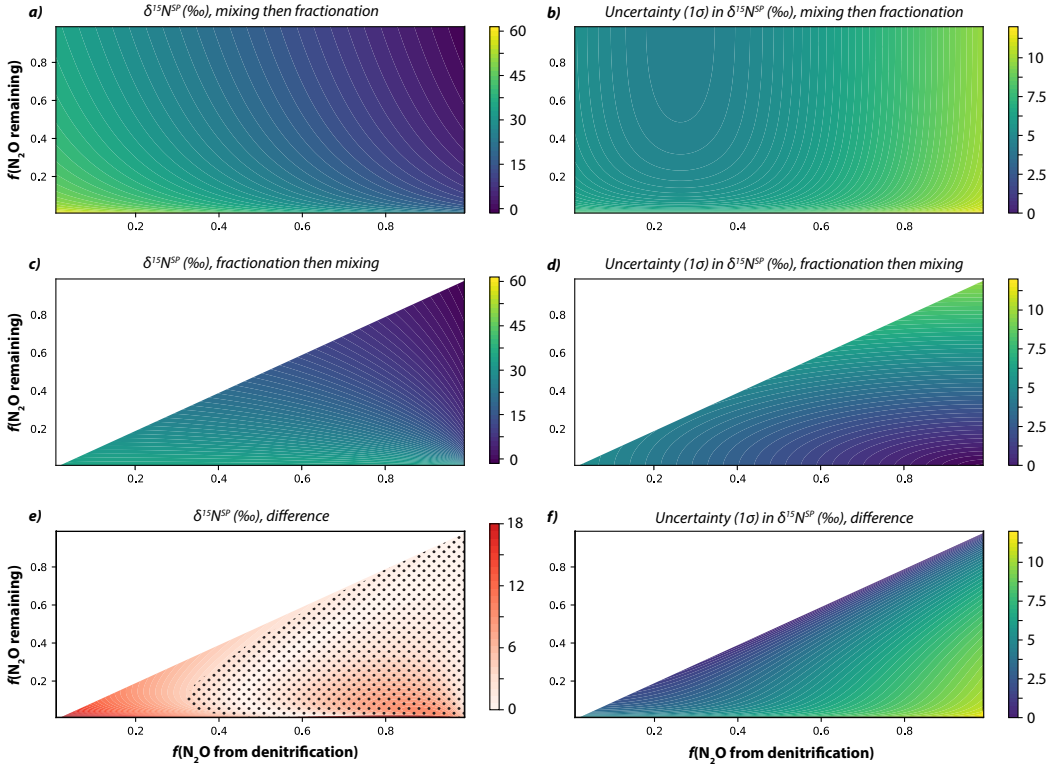

Figure S2. $\delta^{15}N^{SP}$ values simulated across a range of 0 to 1 for the contribution of denitrification to N_2O production (contribution of nitrification = 1 - $f(N_2O$ from denitrification) and 0 to 1 for the fraction of N_2O remaining after consumption. $a)$ and $b)$ show $\delta^{15}N^{SP}$ and its uncertainty simulated with SI Eq. S1. $c)$ and $d)$ show $\delta^{15}N^{SP}$ and its uncertainty simulated with SI Eq. S2. $e)$ and $f)$ show the absolute difference in $\delta^{15}N^{SP}$ between the two simulations and its uncertainty. The dotted region in $e)$ indicates where there is no significant difference between the two scenarios.

S2 Sampling software

Bayesian models can be implemented using different sampling strategies. The most commonly used sampling libraries are `JAGS`, using Gibbs sampling, and `Stan`, using Hamiltonian Monte Carlo sampling. We compared two implementations in three different settings:

- Using the original **stationary** FRAME estimator for one single time step given in Eq. 9 of the main article,
- For the time series model using **independent** time steps described in Eq. 12 of the main article,
- For the **hierarchical** Dirichlet-Gaussian process model described in Eq. 16 of the main article, with joint estimation of the correlation length for source contributions and fractionation.

The general example GenE (Section 2.5.1 of the main article) served as fixed truth value for $\mathbf{f}_t^*$ and r_t^* to apply the models in the above mentioned three settings. The time series were sampled with $N = 64$ points, and for the stationary case the average over time is chosen as fixed value. Each implementation is run for $S = 10000$ sampling steps and the resulting effective sample size, total runtime in seconds and resulting effective samples per second are noted in Table 1. The effective sample sizes are computed using the calculation described by Kruschke (2014) and the reported number are averages over all parameters.

Table S1. Effective sample size, runtime in seconds and effective samples per second for the `Stan` and `JAGS` sampler over $S = 10000$ sampling steps for three different model set ups.

		N_{eff}	Time (s)	N_{eff}/s
Stationary	`Stan`	4 482	10	454
	`JAGS`	5 131	0.5	9 162
Independent	`Stan`	6 350	66	97
	`JAGS`	6 559	22	292
Hierarchical	`Stan`	11 538	1 477	8
	`JAGS`	10	1527	-

`JAGS` outperforms `Stan` for the stationary and independent case by having more effective samples in the shorter amount of time. However, the hierarchical model could only be efficiently sampled by `Stan`, although it took a comparatively long time. These findings are consistent with results on linear models using different numbers of parameters (Beraha et al., 2021). `Stan` appears to be a good option for time series models which inherently have a lot of parameters. The cases where `JAGS` is faster have sufficiently short sampling times for both libraries, therefore `Stan` was used for all subsequent applications.

References

Beraha, M., Falco, D., and Guglielmi, A.: JAGS, NIMBLE, Stan: a detailed comparison among Bayesian MCMC software, pp. 1–46, http://arxiv.org/abs/2107.09357, 2021.

Eyer, S., Tuzson, B., Popa, E., van der Veen, C., Roeckmann, T., Brand, W., Fisher, R., Lowry, D., Nisbet, E., Brennwald, M., Harris, E., Emmenegger, L., Fischer, H., and Mohn, J.: Real-time analysis of δ13C- and δD-CH4 in ambient methane with laser spectroscopy: Method development and first inter-comparison results, Atmospheric Measurement Techniques, 9, 263–280, https://doi.org/10.5194/amt-9-263-2016, 2016.

Kruschke, J.: Doing Bayesian Data Analysis: A Tutorial with R, JAGS, and Stan, Elsevier, 2014.

Röckmann, T., Eyer, S., Van Der Veen, C., Popa, M., Tuzson, B., Monteil, G., Houweling, S., Harris, E., Brunner, D., Fischer, H., Zazzeri, G., Lowry, D., Nisbet, E., Brand, W., Necki, J., Emmenegger, L., and Mohn, J.: In situ observations of the isotopic composition of methane at the Cabauw tall tower site, Atmospheric Chemistry and Physics, 16, 10 469–10 487, https://doi.org/10.5194/acp-16-10469-2016, 2016.

Yu, L., Harris, E., Lewicka-Szczebak, D., and Mohn, J.: What can we learn from N2O isotope data? Analytics, processes and modelling, Rapid Communications in Mass Spectrometry, https://doi.org/10.1002/rcm.8858, 2020.